



# Kent Academic Repository

Hou, Xiaonan, Yousefi Kanani, Armin and Ye, Jianqiao (2018) *Double lap adhesive joint with reduced stress concentration: Effect of slot. Composite Structures*, 202 . pp. 635-642. ISSN 0263-8223.

## Downloaded from

<https://kar.kent.ac.uk/96757/> The University of Kent's Academic Repository KAR

## The version of record is available from

<https://doi.org/10.1016/j.compstruct.2018.03.026>

## This document version

Author's Accepted Manuscript

## DOI for this version

## Licence for this version

CC BY-NC-ND (Attribution-NonCommercial-NoDerivatives)

## Additional information

## Versions of research works

### Versions of Record

If this version is the version of record, it is the same as the published version available on the publisher's web site. Cite as the published version.

### Author Accepted Manuscripts

If this document is identified as the Author Accepted Manuscript it is the version after peer review but before type setting, copy editing or publisher branding. Cite as Surname, Initial. (Year) 'Title of article'. To be published in *Title of Journal*, Volume and issue numbers [peer-reviewed accepted version]. Available at: DOI or URL (Accessed: date).

## Enquiries

If you have questions about this document contact [ResearchSupport@kent.ac.uk](mailto:ResearchSupport@kent.ac.uk). Please include the URL of the record in KAR. If you believe that your, or a third party's rights have been compromised through this document please see our [Take Down policy](https://www.kent.ac.uk/guides/kar-the-kent-academic-repository#policies) (available from <https://www.kent.ac.uk/guides/kar-the-kent-academic-repository#policies>).

# Double lap adhesive joint with reduced stress concentration: effect of slot

Xiaonan Hou\*; Armin Yousefi Kanani; Jianqiao Ye

Department of Engineering, Engineering Building, Lancaster University, Lancaster, LA1  
4YW, UK

\*Corresponding author: x.hou2@lancaster.ac.uk

## **Abstract**

Stress distributions at interfaces of adhesive lap joints have been widely studied to optimize overall structural strength. However, these studies focussed mainly on the mechanics of adhesive layers. In this paper, a novel concept for a double lap adhesive joint is proposed by introducing a slot in its inner adherend. Numerical simulations employing a finite-element method are used to validate the proposed concept. The results show that the introduction of the slots can smooth the stress distributions along the edges of the interfaces between adhesive and adherend and reduce stress concentration near the cut-off ends of the joint. The results also show that the height of the slots has significant effects on alternating the interfacial stresses. Thus, the proposed concept provides a promising way to optimize double lap adhesive joints for enhanced strength with reduced weight.

Key words: Adhesive Joint, Polymers, Mechanical properties, Strength, Finite element analysis (FEA)

## 1 Introduction

In practical engineering applications, there are three basic methods for assembly and joining of engineering components: mechanical joints (e.g. bolted and riveted connections), physical joints (e.g. welds) and chemical joints (e.g. adhesive joints) [1]. Adhesive joints attract more attention due to their advantage of enabling the development of lightweight, cost-effective and highly integrated structures with a more uniform load distribution and improved damage tolerance [2-6]. The configurations of adhesive joints are generally classified as lap joints, butt joints, strap joints, reinforcements, cylindrical joints, T joints and corner joints [7]. Lap joints are usually used for assessing joint strength due to their relatively simple geometric features. Also, lap joints are widely used by researchers to study stress distributions in and failure mechanisms of adhesive bonding [8].

For adhesive lap joints, a uniform stress distribution in the adhesive layer would be ideal for a maximum joint efficiency. However, it is hardly achievable in practical applications due to significant stress concentrations at the ends of the overlaps. Maximum shear stress occurs at the ends of the overlaps, resulting in lower stress in the central regions. Normal (peeling) stress is also concentrated at the ends of the overlaps, usually causing failure of the joint [1, 7, 9-11]. In the last decade, extensive studies on stress concentrations have been performed, showing that they are determined by three main factors: a shear-lag effect, bending induced by non-axial loading and end effects caused by free surfaces at the edges of the adhesive layer [12-15]. Based on this understanding, optimization of stress distribution in adhesive lap joints became one of main focuses of research. To this end, the effects of the geometry of the two components of an adhesive lap joint, i.e., adherend and adhesive, on the interfacial stress distribution were widely studied for improving the overall strength of the joint.

Based on analytical stress models, shear-stress distribution of a thicker adhesive layer should be more uniform, leading to a higher joint strength [9, 16]. However, many studies have shown the opposite [12, 17-20], and that an optimum stress distribution could only be obtained for a range of low thickness of adhesive [17, 18, 21]. This conflict arises from the material properties of adhesive and adherend and the quality of manufacturing process [7, 12]. Concerning the effect of an overlap length of an adhesive layer on the character of stress distribution, some studies demonstrated that concentrated stresses at the ends of the overlap tended to decrease with the increase in its length until reaching a certain magnitude [7, 22, 23]. However, with the increase of the overlap length the stress magnitude in the middle region of the overlap continuously decreases, potentially down to zero for overlaps of certain length. This means that this region does not carry any load [8, 11, 24-26]. Besides, many researches tried to optimize the stress distribution by introducing some specific geometric features to adhesive lap joints. For instance, a spew fillet at the ends of the overlap can effectively reduce the stress concentration, spreading load transfer over a larger area and providing a more uniform shear-stress distribution [12, 27-29]. Research was also carried out to investigate the effect of a discontinuous adhesive layer on the overall joint strength [30-32], which showed that a void or a gap in the adhesive layer could affect the stress distribution in a joint, while had insignificant effect on the overall joint strength [32, 33].

Compared with a large number of studies focussed on adhesive layers, there are only a few works dealing with analysis of the effect of geometric features of adherends on joint strength. As a basic geometric parameter, increased thickness of an adherend could reduce the level of stress concentration at the ends of the overlap, although the weight of the joint increases in this case [19, 34]. Additionally, a novel lap-joint configuration, called a *wavy adherend lap joint*, was developed to optimize the stress distribution in the joint. This configuration effectively reduces stress concentrations and enhances overall joint strength [3, 35, 36]. However, with

the use of such a configuration could increase significantly the extent of complexity of structural design. Another method is to introduce notches to the adherend, which may significantly reduce the maximum peel stress of a lap joint, as showed by numerical simulations [37, 38]. This phenomenon may be due to the increased flexibility of adherend, leading to a better compliance to the deformation of the ends of overlaps. However, the method seems to influence only stresses at the ends of the adherends rather than to change the character of the stress distribution along the entire overlap. According to experimental results, this design showed only a limited influence on the overall strength.

In this paper, a novel configuration of a double lap joint is proposed by embedding a slot in its inner adherend. Using a finite-element method, a stress analysis of this design is performed. The obtained results are then compared with those for the lap joint without the slot, which shows that the introduction of the slot has favourable impact on the stress distributions along its overlaps. By changing the size of the slot, both shear and peel stress distributions along the overlaps of the joint can be tuned, and the stress concentrations at the ends of the overlaps can be reduced, potentially leading to enhanced overall strength of the joint.

## **2 Finite-Element Analysis**

A configuration of a typical double-lap joint, used as a baseline design in this study, is shown in Fig. 1a. The dimensions of the outer adherend are 100 mm  $\times$  25 mm  $\times$  5 mm, representing its length, width and thickness. The dimensions of the inner adherend are 100 mm  $\times$  25 mm  $\times$  10 mm. The length of interface of the double-lap joint is 50 mm, which is also the length of the adhesive layer. The thickness of the adhesive layer is 1 mm and its width is 25 mm. On the basis of this typical joint, a novel double lap joint is developed by embedding a slot in the inner adherend as shown in Fig. 1b. The length of the slot is 45 mm; its width is 25 mm, which is equal to that of the adherends. The height of the slot is  $T$ ; it is used as a variable defining the size of the slot. The position of the slot is fixed at this stage of research. Interface  $ABCD$  is

between the outer adherend and the adhesive layer;  $A'B'C'D'$  is between the inner adherend and the adhesive layer (Fig. 1c). Analysis of stress distributions was conducted along the edges of the interfaces for the double lap joints with and without a slot.

To analyse stress distributions in the double lap joints, 3D finite-element models were developed according to the geometry shown in Fig. 1. However, it is worth noting that the FE models were only developed as a tool for evaluating the new configuration in this work. Hence, there is no specific effort in handling the effects of sharp corners in the configurations, which could induce stress singularities in the calculation. The same boundary conditions were applied to both types of double lap joints, corresponding to the fixture of a specimen in real-life lap shear tests. The surfaces of the ends (left) of outer adherends were fixed using the “ENCASTRE” option in *ABAQUS* FE software, with all the degrees of freedom of the surface constrained:  $U_1=U_2=U_3=UR_1=UR_2=UR_3=0$ . A load of 10 kN was applied on the surface of the inner adherend in the positive  $x$  ( $U_1$ ) direction as shown in Figure 1. To obtain comparable results, the same mesh definition was used in all models of the joints, including the type of elements (linear hexahedron element C3D8R of *ABAQUS*) and their mesh densities (Fig. 2). Elastic material properties were used for both the adherends and the adhesives. The elastic modulus of the adherends was 17500 MPa and the Poisson’s ratio was 0.4, related to a real polymer material (Grivory HTV-5H1: PA6T/6I with 50 % glass fibres). The modulus of the adhesives was 5171 MPa and the Poisson’s ratio was 0.3, representing a typical epoxy adhesive (3M Scotch-Weld 2214). To analyse the effect of the slot, four 3D finite-element models were developed. The models were labelled, respectively, in relation to the size of the slots and where the interfacial stresses were calculated, e.g., either Model-T-U or Model-T-L, where T is the height of the slot in the  $x$ - $y$  plane in millimetres (Fig. 1b); U and L denotes, respectively, upper( $ABCD$ ) and lower ( $A'B'C'D'$ ) interfaces. Four values of T, 0, 1, 2 and 3 mm, were

considered. For instance, Model-0-U is for a traditional double lap joint without any slot, and shows stress distributions along the edge of its upper interface.

### 3 Stress Distributions

Stress distributions in interfaces  $ABCD$  and  $A'B'C'D'$  were calculated using the developed FE models. Elements along the two edges ( $AB$  and  $A'B'$ ) were used in the analysis to include the free end effects and effects of singularity (at points  $A$ ,  $B$ ,  $A'$  and  $B'$ ) in the FE method. Obviously, edges  $CD$  and  $C'D'$  are equivalent to  $AB$  and  $A'B'$  due to the symmetry. As shown in Figure 3-6, the models of the typical double lap joint (Model-0-U/L) give the typical stress distributions along  $AB$  and  $A'B'$  edges of the interfaces for both shear stress ( $\tau_{xy}$ ) and peel stress ( $\sigma_{yy}$ ). The results show that the developed finite-element models can describe the trends of the stress distributions in double lap joints satisfactorily.

The distributions of shear stresses ( $\tau_{xy}$ ) along edge  $AB$  in the upper interface ( $ABCD$ ) are shown in Fig. 3. A parabolic stress distribution is obtained with Model-0-U, typical for a conventional double lap joint. Apparently, high stress levels are obtained around the two ends of the edge, with lower stress concentrations in the middle portion of the overlap. On the basis of the trend of the distribution, the overlap is divided into three sections for analysis for all the models, as shown in Fig. 3a. In section I (Fig. 3b), it is obvious that the stress levels of the models with rectangular slots (Model-1-U, Model-2-U and Model-3-U), are generally lower than that of the model without a slot (Model-0-U). The peak stresses of all the models are obtained at position  $x = 0.75\text{mm}$ . For Model-0-U, the magnitude of the negative peak stress is  $-13.3\text{ MPa}$ , the highest among all the models. For the models with slots, the stress concentration in section I decreases with the increase of the height of the slot. The magnitudes of the negative peak stresses at position  $x = 0.75\text{mm}$  are  $-12.3$ ,  $-11.90$  and  $-11.4\text{ MPa}$ , respectively. Compared with Model-0-U the differences are  $7.5\%$ ,  $10.5\%$  and  $14.3\%$ , which show effective reduction in stress concentration. In section II (Fig. 3c), a significant difference is shown between the

standard double lap joint and the double lap joints with slots. In the middle section of the edge  $AB$ , more even stress distributions are obtained in the models with slots, compared with the parabolic stress distribution of the model without a slot. The phenomenon means that shear stress is transferred from the ends of the overlap to its middle section. The average shear stress of the model without a slot (Model-0-U) is -2.4 MPa. For Model-1-U, Model-2-U and Model-3-U, the magnitudes are -4.1, -4.2 and -4.4 MPa, respectively. Compared with Model-0-U, the differences are 70.8 %, 75.0 % and 83.3 %. The results show that more stresses are distributed along this section with the increase in the height of the slot. In section III (Fig. 3d), the stress levels are clearly reduced in the models with slots (Model-1-U, Model-2-U and Model-3-U) compared to the model without a slot (Model-0-U). The stresses at the position ( $x = 48.75\text{mm}$ ) are the negative peak stresses for all the models. The peak stress of Model-0-U is -12.5 MPa. For other models, the magnitudes are similar, which are -10.8, -10.9 and -11.1 MPa for Model-1-U, Model-2-U and Model-3-U, respectively. However, comparing with section I, the effect of the height of the slot on the stress concentration is reversed. The differences in stress concentrations are 13.6 %, 12.8% and 11.2%. With the increase of the height of the slot, the effect of the slot is reduced. The phenomenon indicates that the height of the slot has different effects on the stresses at different ends of the overlap.

In the lower interface ( $A'B'C'D'$ ), the distributions of shear stresses ( $\tau_{xy}$ ) are obtained along edge  $A'B'$ , which is similar to that of edge  $AB$  of the upper interface ( $ABCD$ ), although the positions and magnitudes of the peak stresses are slightly different. Model-0-L shows a typical parabolic stress distribution and high stress levels are obtained around the two ends of the edge (Fig 4a). The models with slots (Model-1-L, Model-2-L and Model-3-L) generally show lower stress concentration levels compared to the model with a slot (Model-0-L). In section I (Fig.4b), the negative peak stress of Model-0-L is obtained at position  $x = 1.75 \text{ mm}$ , which is -12.2 MPa. For the models with slots, the peak stresses are obtained at position  $x = 1.25 \text{ mm}$ , and the

magnitudes are -10.9 MPa, -10.4 MPa and -9.8 MPa, respectively. The respective reductions are 10.7%, 14.8 % and 19.7 % in comparison with Model-0-L. In section II (Fig.4c), shear stresses are distributed more evenly in the models with slots, which means more stresses can be carried. The average shear stresses of the models are -2.4 MPa, -4.1 MPa, -4.2 MPa and -4.3 MPa, respectively, for Model-0-L, Model-1-L, Model-2-L and Model-3-L. Compared to Model-0-L, the models with slots carry 70.8%, 75.0 % and 79.2 % more shear stresses in this section. In section III (Fig. 4d), the negative peak shear stress of Model-0-L is obtained at position  $x = 49.25$  mm, which is -13.8 MPa. For the models with slots, the position of negative peak stresses is at  $x = 49.75$  mm, and the magnitudes are -12.9 MPa, -13.3 MPa and -13.9 MPa for Model-1-L, Model-2-L and Model-3-L. Compared to Model-0-L, the peak stresses are reduced by 6.5 % and 3.6 % and increased by 0.7%, respectively. The comparisons show that the slot still reduces the level of stress concentration at this end of the edge, when the height of the slot is properly defined.

Normal stress ( $\sigma_{yy}$ ) affects overall strength of the joint significantly, since it usually dominates failure of adhesive lap joints. Figure 5a demonstrates distributions of normal stresses along edge  $AB$  of the upper interface ( $ABCD$ ). For Model-0-U, which presents a typical double lap joint, a classical stress distribution is obtained. Peak stresses are at the two ends of the overlap as shown in sections I and III, whilst a relatively even stress distribution is obtained in section II. For the models with the embedded slots (Model-1-U, Model-2-U and Model-3-U), similar stress distributions to Model-0-U are obtained. However, the effect of stress concentrations is significantly reduced. As shown in Fig.5b for section I, the peak stresses of all the models are negative, which means that this end of the overlap is under compression. The peak stress of the typical double lap joint (Model-0-U) is -10.9 MPa at position  $x = 0.75$  mm, which represents the highest stress concentration among all the models. For the models with slots, the negative peak stresses are -9.1, -8.4 and -7.6 MPa at the same position  $x = 0.75$  mm, respectively,

representing reductions of 16.5 %, 22.9 % and 30.3 %. Apparently, the effect of stress concentration is reduced with the increase of the height of the slots. In section II (Fig. 5c), nearly constant stresses are distributed along the overlap  $AB$  for the models with slots. However, the stress level obtained in the model without a slot changes from positive to negative (2.5 to -2.1 MPa) along the overlap (from 10 to 40 mm), which results in a bending moment acting on this section. For the models with slots, the stresses are positive and remain almost constant at a relatively low level within this section of the overlap. The results show no bending in the models with the slots. The stress levels in the models increase with the increase in the height of slots. The average stresses are 0.23, 0.25 and 0.27 MPa for Model-1-U, Model-2-U and Model-3-U, respectively. In section III (Fig. 5d) of overlap  $AB$ , the peak stresses are located at position  $x = 49.25$  mm for all the models, the magnitudes are positive, which indicates peel stresses. The highest stress of 8.6 MPa is obtained in the model without a slot. For the models with slots, the peak stresses are significantly lower. And the peak stresses decrease with the increased height of the slots, which indicate an effective reduction in stress concentration. The stresses are 5.3, 4.6 and 3.7 MPa at position  $x = 49.25$  mm for Model-1-U, Model-2-U and Model-3-U, respectively, i.e. are 38.4 %, 46.5 % and 57.0 % lower. From the results, it is also observed that the normal stresses in Model-0-U change from negative (compression) to positive (peel) in this section, indicating bending of this part. However, the stress distributions in the models with slots show smoother changes in their magnitudes, which may contribute to reduction in stress concentration.

Figure 6a shows normal stress ( $\sigma_{yy}$ ) distributions along edge  $A'B'$  of interface  $A'B'C'D'$ . Compared with the distributions along edge  $AB$ , a similar trend is obtained. As shown in section I (Fig. 6b), the peak negative stresses are all obtained at position  $x = 0.25$  mm. The highest compressive stress is obtained from Model-0-L, which is -9.1 MPa. For the models with slots (Model-1-L, Model-2-L and Model-3-L), the negative peak stresses are -6.8, -6.0 and -5.1 MPa,

respectively. Compared to Model-0-L, the reductions are 25.3%, 34.1% and 44%. In section II (Fig.6c), a significant bending moment occurs in the model without a slot (Model-0-L), the stress decreases from 3.6 to -3.1MPa. For models with slots, constant stress distributions are obtained at very low stress levels. The average stresses are 0.24, 0.26 and 0.27 MPa, respectively. In section III of the edge (Fig. 6d), the peak peel stresses are all located at position  $x = 49.75$  mm. The stresses in the models with slots (Model-1-L, Model-2-L and Model-3-L) are 9.4, 8.0, and 6.3 MPa, respectively. They are significantly lower than the magnitude in Model-0-L, which is 15.7 MPa at the same position. The differences are 40.1%, 49.0% and 59.9 %.

#### **4 Mechanical Properties**

The inner adherend of a double lap joint is one of the major structural components, and its effective stiffness is reduced when a slot is introduced. Consequently, overall stiffness of the joint is lower. To understand this effect, overall mechanical properties of the joints are analysed based on the developed FE models. The strain is calculated according to the displacement of the loading end of the inner adherend and the overall length of the joint under applied force (Fig.1a). The stress is calculated using the applied force and the area of the surface of the end of the inner adherend. The moduli of all the models are then calculated and presented in Table 1. It is shown that an embedding slot causes a reduction in overall stiffness of the double lap joint. Under a 10 kN loading, the models with slots experiences larger strains and their moduli are lower compared with those in the model without a slot. Referring to the volume fractions of the slots,  $R_s$  (volume of the slot to the volume of the joint without a slot), the models with higher  $R_s$  shows lower modulus. The modulus of Model-1-U/L ( $R_s = 2.1\%$ ) is 2.1% lower than that in Model-0-U/L ( $R_s = 0\%$ ). With an increase of  $R_s$ , the modulus generally decreases. For Model-2-U/L and Model-3-U/L, the reductions are 3.8 % and 5.8 % compared to Model-0-U/L, respectively.

## 5 Discussion and Conclusions

In this paper, a novel configuration of a double lap adhesive joint has been proposed by introducing a slot in its inner adherend. Using the finite-element method, stress distributions along the edges of both upper and lower interfaces were analysed. Firstly, a conventional double lap joint was analysed, showing the well-known stress distributions along the edges of the interfaces between the adhesive and adherends. Then the joints with slots were analysed to demonstrate redistribution of interfacial stresses and reductions in stress concentrations along the edges of the interfaces, which could potentially affect overall strength of the joint. Moreover, the results of the parametric FE analysis indicated that the effects of the slot could be tuned by adjusting its geometric parameters, such as the height of the slot. Based on the obtained results, the following discussion and conclusions can be drawn:

### (a) For the embedding slot:

The concept of this study is to change the effective mechanical properties of the inner adherend of a double lap joint by embedding a slot. The section of the inner adherend with the slot is divided into two separated struts with the slot between them (Fig. 1b). With the slot, the mechanical properties of the inner adherend become discontinuous. Consequently, its deformation mechanism changes, affecting overall mechanical properties of the double lap joint.

According to the obtained results of the FE simulations, the slot could effectively change the character of stress distribution along the edges of the interfaces between the adhesive and adherends. The stresses along the two edges ( $AB$  and  $A'B'$ ) were analysed. Along the edges, shear stresses ( $\tau_{xy}$ ) in the models with slots were transferred from the ends of the overlaps to the middle sections compared with the model without a slot. The results also showed that the stress concentrations around the ends of the overlaps were reduced. This is caused by the reduced effective stiffness of the section of the inner adherend with a slot. When the joint is

loaded, higher shear strains occurs along the loading direction in this section. It means that relatively higher shear stresses are generated along the overlaps, and the stress concentrations at the ends of the edges are then reduced. Moreover, even stress distributions are obtained in the middle sections of the overlaps in the models with slots, and the average stress levels are significantly higher than the one in the model without a slot, which suggests that the strength of a joint with a slot could be enhanced continuously by increasing the length of its overlap.

For the distribution of normal stress ( $\sigma_{yy}$ ), the maximum stress concentrations also occur at the ends of the overlaps, and the embedding slot can also reduce their levels. Moreover, the eccentric bending moment, which usually occurs in the model without a slot, is also reduced. This behaviour can be explained in terms of the increased effective Poisson's ratio of the section with a slot. Since the section is divided by the slot into two separated struts on either sides of the neutral axial, local bending moments could occur at either struts, which are induced by the discontinuous mechanical properties between the different sections of the inner adherend. Under the external loading, the section with a slot would contract more significantly along the transverse direction of loading compared to the sections without a slot, which indicates a higher effective Poisson's ratio at this section. Since the peel stress of a double lap joint is generally caused by the overall bending moment based on its geometric configuration, the local bending moments induced by the slot could potentially compensate the effect of the overall bending moment and reduce the peel-stress concentration.

The height of slot was used as a controlling parameter in this study. It was observed that it affected the magnitudes of stress concentrations of the proposed double lap joint. According to the results, the maximum stress concentrations in the interfaces occur at the two ends of the overlaps. In section I of the overlaps, the shear stress ( $\tau_{xy}$ ) concentrates decrease with the increase of the height of the slots (Fig. 3b and 4b). A similar trend is observed for normal stress ( $\sigma_{yy}$ ) concentrations (Fig. 5b and 6b). At the other end of the overlaps (section III), the peak

shear stresses ( $\tau_{xy}$ ) increase as the height of the slots increases, while the magnitudes still can be lower than that from the model without a slot, if the dimensions of the slot are properly defined (Fig. 3d and 4d). The trend is different from the one in section I. The results show that the height of the slot has different effects on the shear stress ( $\tau_{xy}$ ) concentrations at the two ends of the overlaps. The effect of the slot on normal stress ( $\sigma_{yy}$ ) concentrations in section III is the same as that in section I, i.e., the stress concentration decreases, as the height of the slots increases.

(b) For the interfaces:

Both the upper and lower interfaces ( $ABCD$  and  $A'B'C'D'$ ) of the joints were analysed. The results showed that the effect of slot on stress distributions along the edges of both interfaces were similar (Fig. 3a, 4a, 5a and 6a). However, the magnitudes of the peak stresses are different at different interfaces (Table 2). In section I, the magnitudes of peak stresses ( $\tau_{xy}$  and  $\sigma_{yy}$ ) in the upper interface are higher than the ones obtained in the lower interface. The difference may be attributed to the different constraints at the vertexes of the interfaces. Point  $A$  in the upper interface is a vertex of a sharp re-entrant corner with a  $90^\circ$  external angle, which can induce higher stress concentrations in its vicinity. Whilst, point  $A'$  in the lower interface is located on a free edge [39, 40]. The stress concentrations around this point are more dominated by the alternative material properties in the interface. In section III, a similar trend was observed. The magnitudes of peak stresses ( $\tau_{xy}$  and  $\sigma_{yy}$ ) around point  $B'$  (lower interface), which is a vertex of a re-entrant corner, are higher than the ones obtained around point  $B$  (upper interface), which is located on a free edge.

(c) Stiffness and strength of overall double lap joint:

The embedded slot in the developed double lap joint reduces effective stiffness of the inner adherend and, consequently, decreases the overall stiffness of the double joint along the loading direction. However, joint strength is a more important property for a double lap joint.

According to the obtained results, the embedded slot can effectively reduce both shear and peel stress concentrations in the interfaces of the joint, especially the latter, if the dimension of the slot are properly designed. As a result, the overall joint strength could be potentially enhanced, resulting in a stronger joint. Moreover, it is also worthy of noting that the overall weight of the adhesive double lap joint is reduced at almost the same rate as the overall stiffness is reduced, meaning that the ratio of mechanical performance to weight is retained.

The major contribution of this paper is to present a new design concept that could enhance the strength of an adhesive lap joint by introducing an imperfection into its structural component. Based on this concept, further studies are required to explore further to investigate, such as, slots with varying dimensions/shapes, slots in different positions, adherends with different properties (multi-material joint) and different loading conditions. When the effects of these factors are clearly understood, optimization could be implemented to develop adhesive joints with enhanced strength and lighter weight according to specific requirements of real engineering applications.

## Reference

- [1] Adams RD, Comyn J, Wake WC. Structural Adhesive Joints in Engineering. 2nd ed. London, UK: Chapman & Hall, 1997.
- [2] Li G, Pang S-S, Woldesenbet E, Stubblefield MA, Mensah PF, Ibekwe SI. Investigation of prepreg bonded composite single lap joint. *Composites Part B: Engineering*. 2001;32:651-8.
- [3] Ávila AF, Bueno PndO. An experimental and numerical study on adhesive joints for composites. *Composite Structures*. 2004;64:531-7.
- [4] Banea MD, Da Silva LFM. Adhesively bonded joints in composite materials: An overview. *Proceedings of the Institution of Mechanical Engineers, Part L: Journal of Materials Design and Applications*. 2009;223:1-18.
- [5] Ghosh PK, Kumar K, Preeti P, Rajoria M, Misra N. Superior dissimilar adhesive joint of mild steel and aluminium using UDM processed epoxy based TiO<sub>2</sub> nano-filler composite adhesive. *Composites Part B: Engineering*. 2016;99:224-34.
- [6] Hayes-Griss JM, Gunnion AJ, Afaghi Khatibi A. Damage tolerance investigation of high-performance scarf joints with bondline flaws under various environmental, geometrical and support conditions. *Composites Part A: Applied Science and Manufacturing*. 2016;84:246-55.
- [7] Da Silva LFM. Design Rules and Methods to Improve Joint Strength. In: Da Silva LFM, Öchsner A, Adams R, editors. *Handbook of Adhesion Technology*: Springer Berlin Heidelberg; 2011. p. 689-723.
- [8] States DN, DeVries KL. Geometric Factors Impacting Adhesive Lap Joint Strength and Design. *Journal of Adhesion Science and Technology*. 2012;26:89-107.
- [9] Volkersen O. Die Nietkraftverteilung in Zugbeanspruchten Nietverbindungen mit Konstanten Laschenquerschnitten. *Luftfahrtforschung*. 1938;15:7.
- [10] Sneddon I. The distribution of stress in adhesive joints. In: Eley DD, editor. *Adhesion*. London: Oxford University Press; 1961.

- [11] Vallée T, Correia JR, Keller T. Optimum thickness of joints made of GFPR pultruded adherends and polyurethane adhesive. *Composite Structures*. 2010;92:2102-8.
- [12] Adams RD, Peppiatt NA. Stress analysis of adhesive-bonded lap joints. *The Journal of Strain Analysis for Engineering Design*. 1974;9:185-96.
- [13] Hart-Smith LJ. Adhesive bonded double lap joints. Hampton, Virginia: NASA; 1973.
- [14] Tsai MY, Morton J. An investigation into the stresses in double-lap adhesive joints with laminated composite adherends. *International Journal of Solids and Structures*. 2010;47:3317-25.
- [15] Zhang D, Ye J, Lam D. Ply cracking and stiffness degradation in cross-ply laminates under biaxial extension, bending and thermal loading. *Composite Structures*. 2006;75:121-31.
- [16] Goland M, Reissner E. The Stresses in Cemented Joints. *Journal of Applied Mechanics*. 1944;2:10.
- [17] Da Silva LFM, Rodrigues TNSS, Figueiredo MAV, de Moura MFSF, Chousal JAG. Effect of Adhesive Type and Thickness on the Lap Shear Strength. *The Journal of Adhesion*. 2006;82:1091-115.
- [18] Gleich DM, Van Tooren MJL, Beukers A. Analysis and evaluation of bondline thickness effects on failure load in adhesively bonded structures. *Journal of Adhesion Science and Technology*. 2001;15:1091-101.
- [19] Aydin MD, Özel A, Temiz Ş. The effect of adherend thickness on the failure of adhesively-bonded single-lap joints. *Journal of Adhesion Science and Technology*. 2005;19:705-18.
- [20] Li G, Lee-Sullivan P, Thring RW. Nonlinear finite element analysis of stress and strain distributions across the adhesive thickness in composite single-lap joints. *Composite Structures*. 1999;46:395-403.

- [21] Van Tooren MJL, Gleich DM, Beukers A. Experimental verification of a stress singularity model to predict the effect of bondline thickness on joint strength. *Journal of Adhesion Science and Technology*. 2004;18:395-412.
- [22] Campilho RDSG, De Moura MFSF, Domingues JJMS. Modelling single and double-lap repairs on composite materials. *Composites Science and Technology*. 2005;65:1948-58.
- [23] De Castro J, Keller T. Ductile double-lap joints from brittle GFRP laminates and ductile adhesives, Part I: Experimental investigation. *Composites Part B: Engineering*. 2008;39:271-81.
- [24] Keller T, Vallée T. Adhesively bonded lap joints from pultruded GFRP profiles. Part I: stress-strain analysis and failure modes. *Composites Part B: Engineering*. 2005;36:331-40.
- [25] Masmanidis IT, Philippidis TP. Progressive damage modeling of adhesively bonded lap joints. *International Journal of Adhesion and Adhesives*. 2015;59:53-61.
- [26] Anyfantis KN. On the failure analysis of bondlines: Stress or energy based fracture criteria? *Engineering Fracture Mechanics*. 2014;126:108-25.
- [27] F M da Silva L, D Adams R. Techniques to reduce the peel stresses in adhesive joints with composites. *International Journal of Adhesion and Adhesives*. 2007;27:227-35.
- [28] Akpınar S, Doru MO, Özel A, Aydın MD, Jahanpasand HG. The effect of the spew fillet on an adhesively bonded single-lap joint subjected to bending moment. *Composites Part B: Engineering*. 2013;55:55-64.
- [29] Lang TP, Mallick PK. Effect of spew geometry on stresses in single lap adhesive joints. *International Journal of Adhesion and Adhesives*. 1998;18:167-77.
- [30] Rossettos JN, Zang E. On the Peak Shear Stresses in Adhesive Joints With Voids. *Journal of Applied Mechanics*. 1993;60:559-60.
- [31] Shishesaz M, Bavi N. Shear stress distribution in adhesive layers of a double-lap joint with void or bond separation. *Journal of Adhesion Science and Technology*. 2012;27:1197-225.

- [32] De Moura MFSF, Daniaud R, Magalhães AG. Simulation of mechanical behaviour of composite bonded joints containing strip defects. *International Journal of Adhesion and Adhesives*. 2006;26:464-73.
- [33] Pinto AMG, Ribeiro NFQR, Campilho RDSG, Mendes IR. Effect of Adherend Recessing on the Tensile Strength of Single Lap Joints. *The Journal of Adhesion*. 2013;90:649-66.
- [34] Kim H. The influence of adhesive bondline thickness imperfections on stresses in composite joints. *The Journal of Adhesion*. 2003;79:621-42.
- [35] Fessel G, Broughton JG, Fellows NA, Durodola JF, Hutchinson AR. Evaluation of different lap-shear joint geometries for automotive applications. *International Journal of Adhesion and Adhesives*. 2007;27:574-83.
- [36] Ávila AF, Bueno PndO. Stress analysis on a wavy-lap bonded joint for composites. *International Journal of Adhesion and Adhesives*. 2004;24:407-14.
- [37] Sancaktar E, Simmons SR. Optimization of adhesively-bonded single lap joints by adherend notching. *Journal of Adhesion Science and Technology*. 2000;14:1363-404.
- [38] Cognard JY, Badulescu C, Maurice J, Créac'hcadec R, Carrère N, Vedrine P. On modelling the behaviour of a ductile adhesive under low temperatures. *International Journal of Adhesion and Adhesives*. 2014;48:119-29.
- [39] Zhang D, Ye J, Lam D. Free-Edge and Ply Cracking Effect in Angle-Ply Laminated Composites Subjected to In-Plane Loads. *Journal of Engineering Mechanics*. 2007;133:1268-77.
- [40] Zhang D, Ye J, Sheng HY. Free-edge and ply cracking effect in cross-ply laminated composites under uniform extension and thermal loading. *Composite Structures*. 2006;76:314-25.

## Figure Captions

Figure 1: Configurations of double lap joints and boundary conditions (Unit: mm): (a) without slot (typical); (b) with slot; (c) interfaces between adhesive and adherends

Figure 2: Finite element meshes of a double lap joint with a slot

Figure 3: Distributions of shear stress ( $\tau_{xy}$ ) along edge  $AB$ : (a) overview; (b) section I; (c) section II; (d) section III

Figure 4: Distributions of shear stress ( $\tau_{xy}$ ) along edge  $A'B'$ : (a) overview; (b) section I; (c) section II; (d) section III

Figure 5: Distributions of peel stress ( $\sigma_{yy}$ ) along edge  $AB$ : (a) overview; (b) section I; (c) section II; (d) section III

Figure 6: Distributions of peel stress ( $\sigma_{yy}$ ) along edge  $A'B'$ : (a) overview; (b) section I; (c) section II; (d) section III

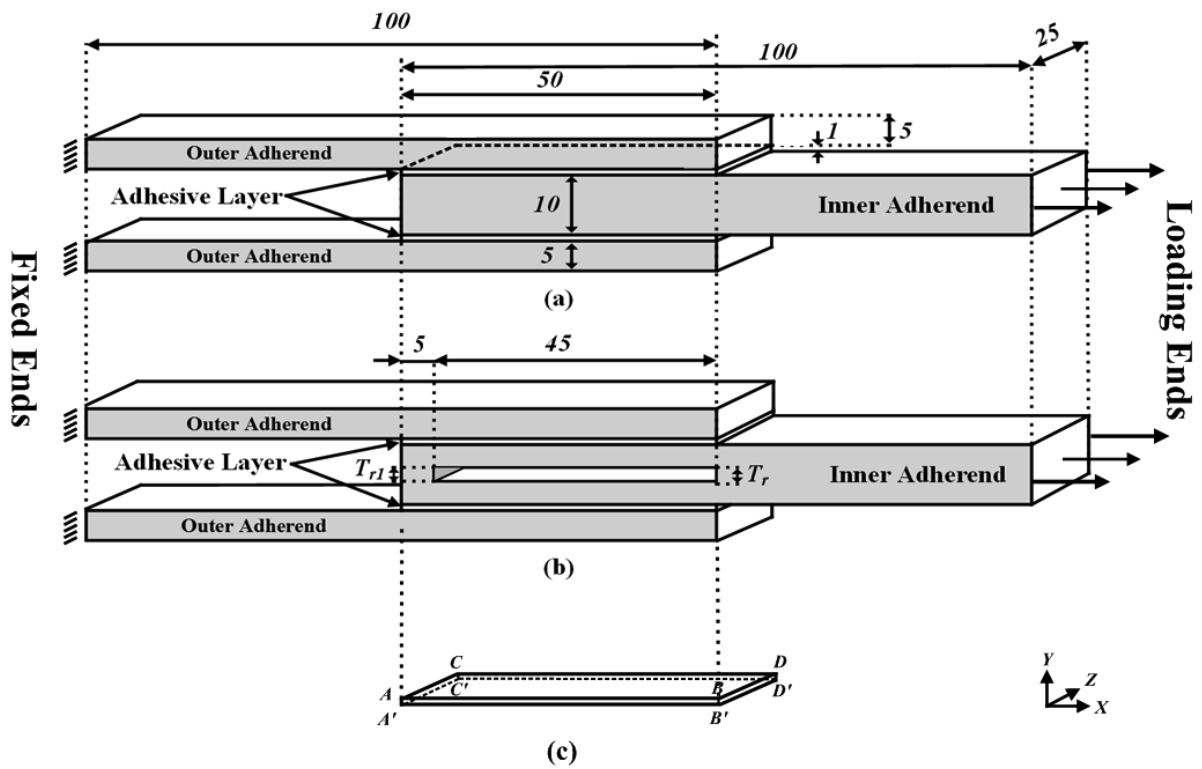


Figure 1: Configurations of double lap joints and boundary conditions (Unit: mm): (a) without slot (typical); (b) with slot; (c) interfaces between adhesive and adherends

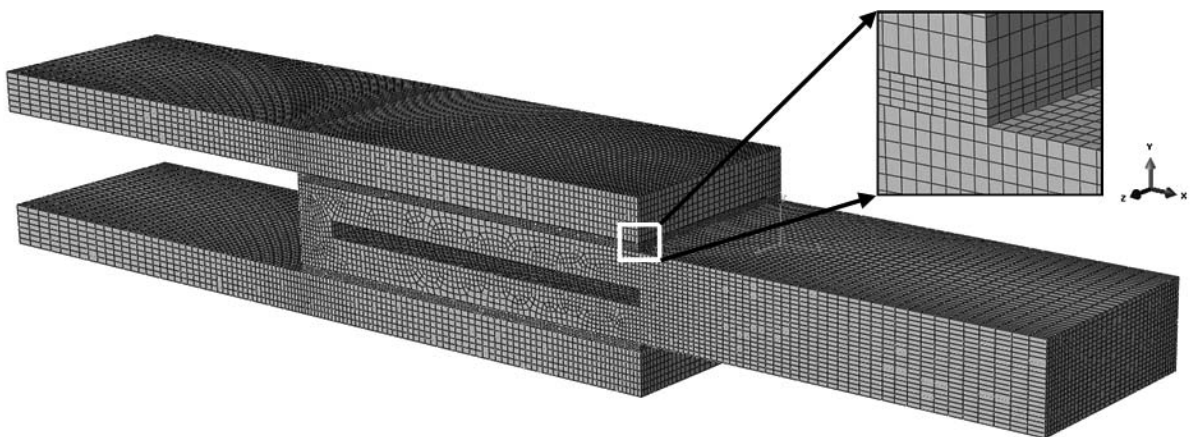


Figure 2: Finite element meshes of a double lap joint with a slot

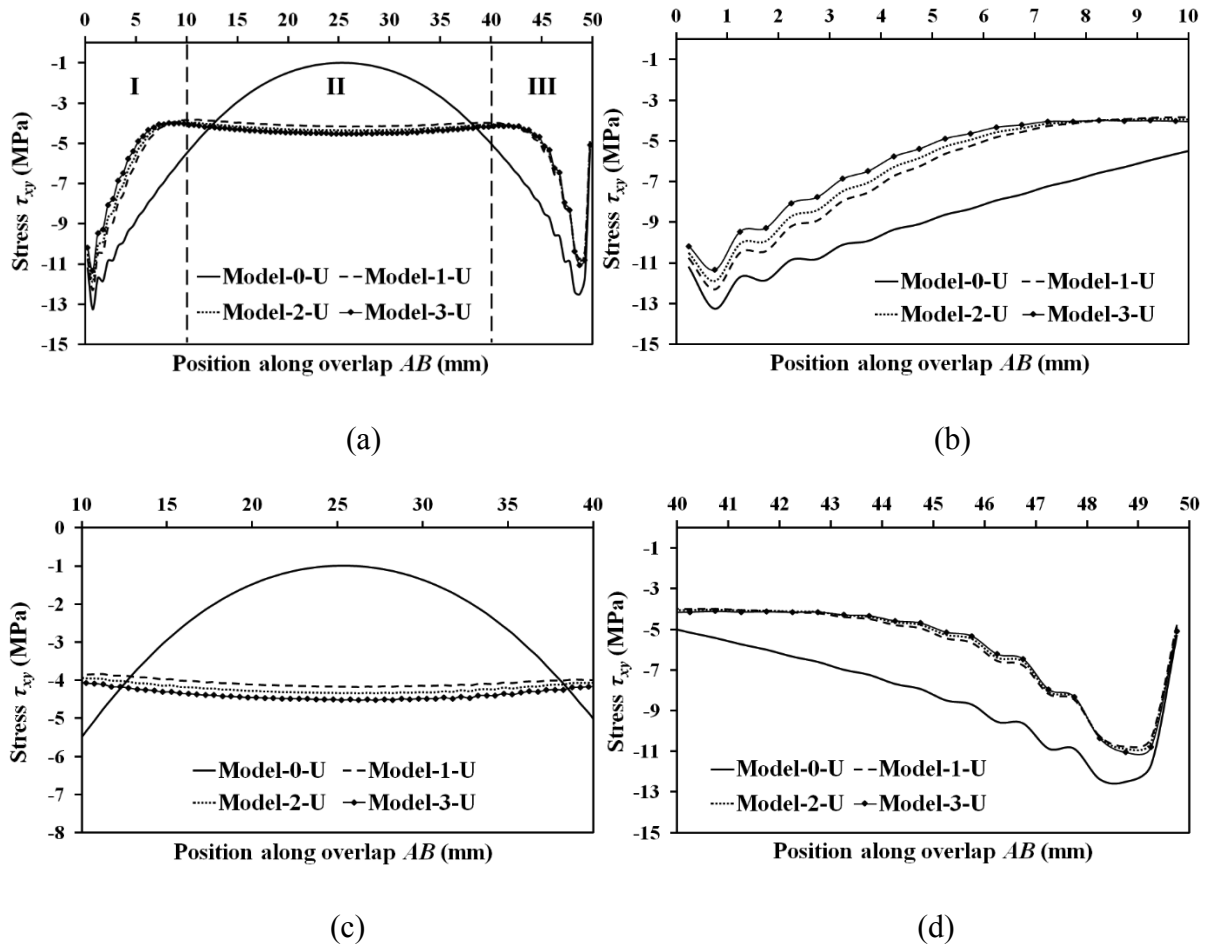


Figure 3: Distributions of shear stress ( $\tau_{xy}$ ) along edge AB: (a) overview; (b) section I; (c) section II; (d) section III

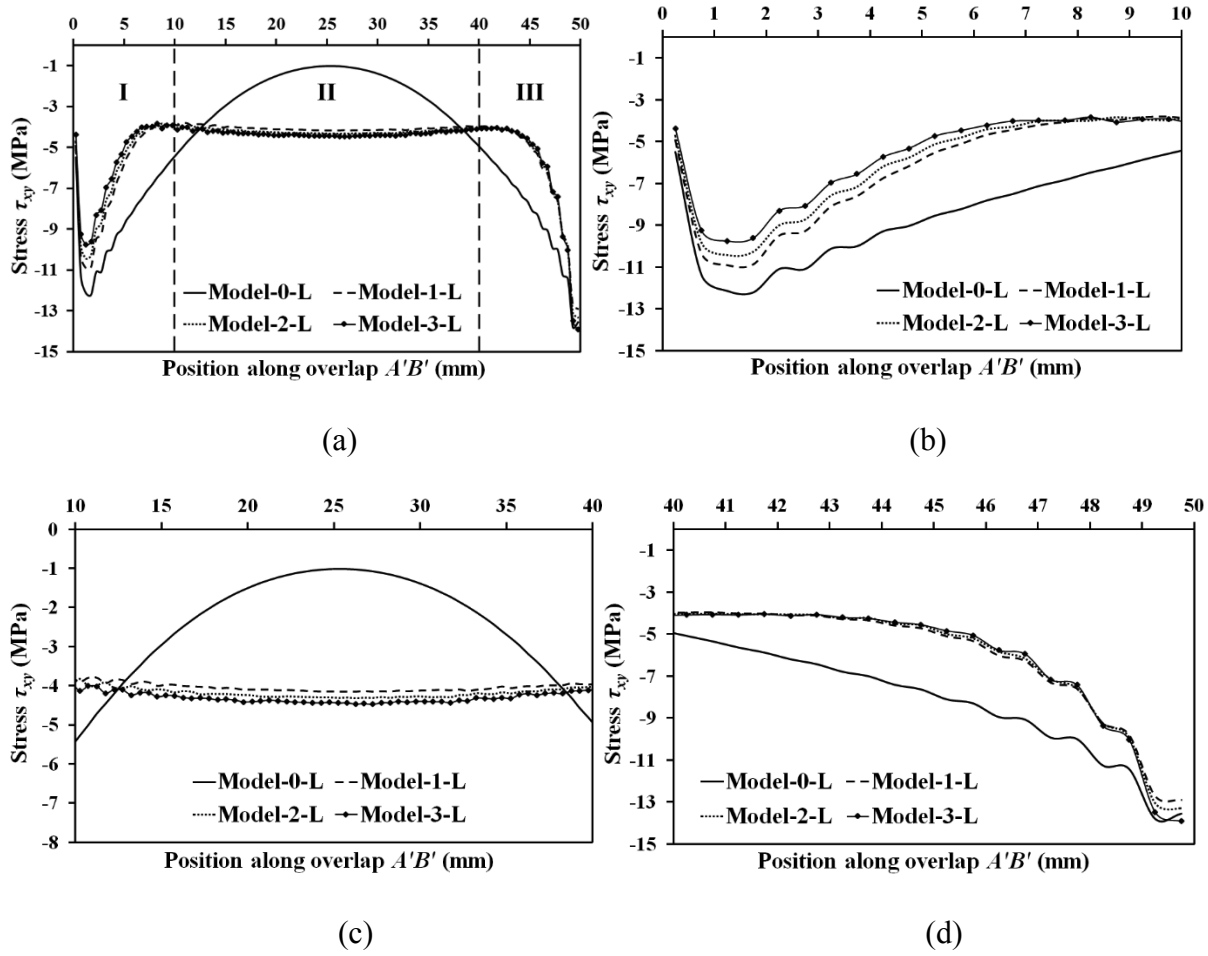


Figure 4: Distributions of shear stress ( $\tau_{xy}$ ) along edge  $A'B'$ : (a) overview; (b) section I; (c) section II; (d) section III

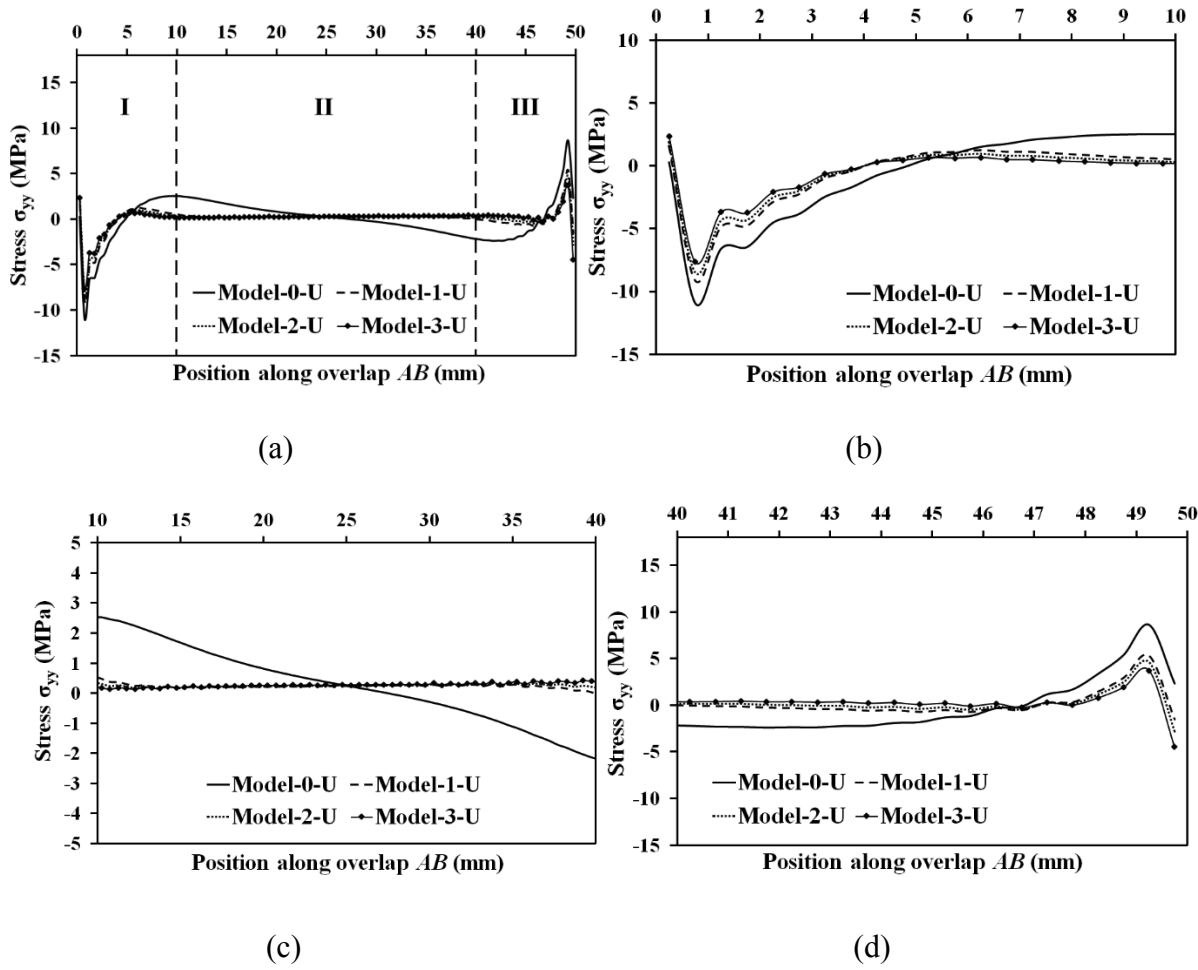


Figure 5: Distributions of peel stress ( $\sigma_{yy}$ ) along edge  $AB$ : (a) overview; (b) section I; (c) section II; (d) section III

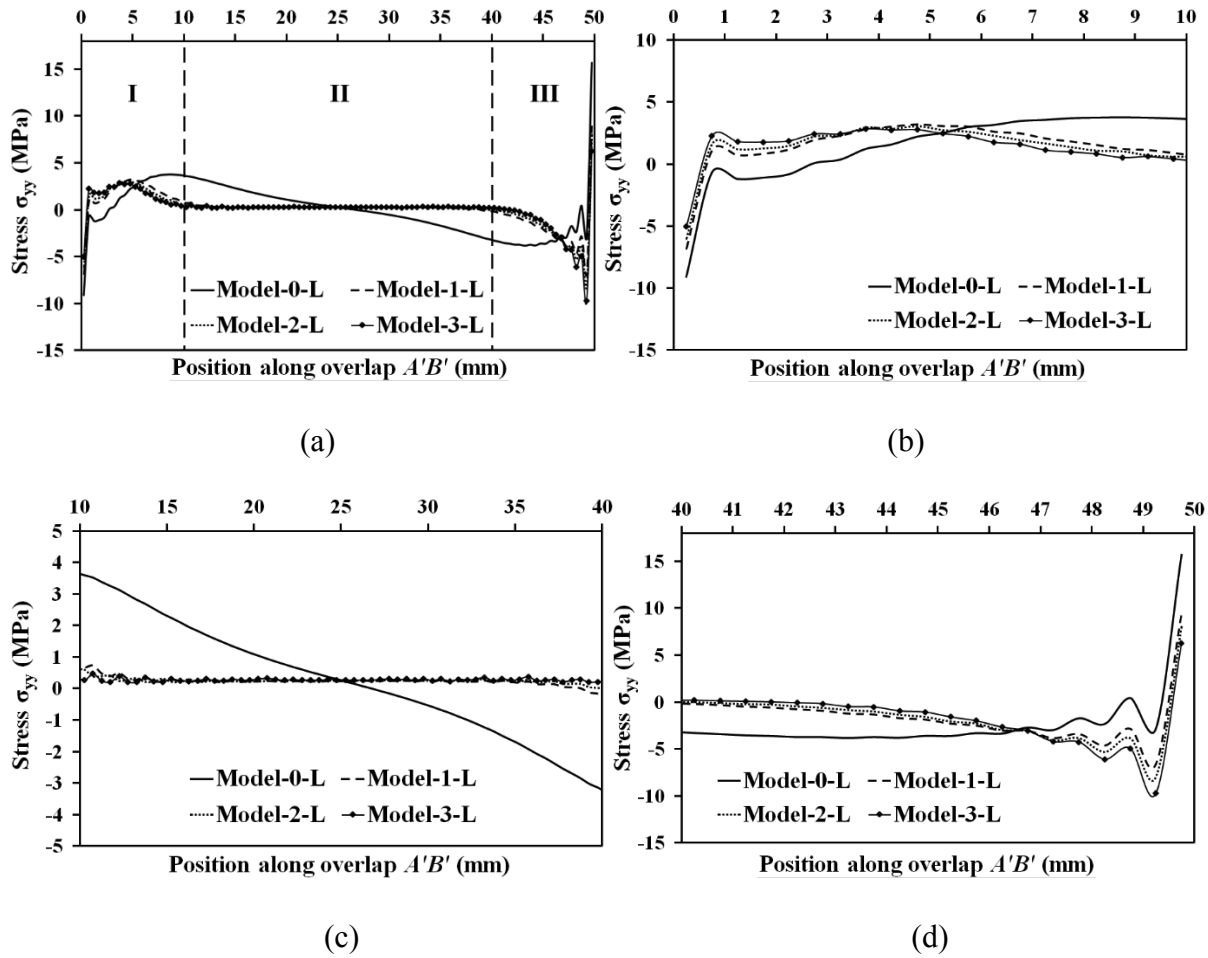


Figure 6: Distributions of peel stress ( $\sigma_{yy}$ ) along edge  $A'B'$ : (a) overview; (b) section I; (c) section II; (d) section III

Table 1: Mechanical properties of double lap joints

Model Code	Model-0- (U/L)	Model-1- (U/L)	Model-2- (U/L)	Model-3- (U/L)
Modulus (MPa)	20182.9	19754.5	19421.1	19015.9
Strain (%) under 10 kN	0.198	0.203	0.206	0.210
Volume fraction of slot (%) in volume of overall joint Rs	0	2.1	4.3	6.4

Table 2: Comparisons of peak stresses between upper and lower interfaces

Model Code	Model-0-(U/L)	Model-1-(U/L)	Model-2-(U/L)	Model-3-(U/L)
Interface	Upper/Lower	Upper/Lower	Upper/Lower	Upper/Lower
Peak shear stress ( $\tau_{xy}$ ) (MPa) in section I	-13.3/-12.2	-12.3/-10.9	-11.9/10.4	-11.4/-9.8
Peak normal stress ( $\sigma_{yy}$ ) (MPa) in section I	-10.9/-9.1	-9.1/-6.8	-8.4/-6.0	-7.6/-5.1
Peak shear stress ( $\tau_{xy}$ ) (MPa) in section III	-12.5/-13.8	-10.8/-12.9	-10.9/-13.3	-11.1/-13.9
Peak normal stress ( $\sigma_{yy}$ ) (MPa) in section III	8.6/15.7	5.3/9.4	4.6/8.0	3.7/6.3